

The nature of spectral gaps due to pair formation

T. Micklitz¹ and M. R. Norman¹

¹*Materials Science Division, Argonne National Laboratory, Argonne, IL 60439*

(Dated: February 13, 2022)

Several phenomenological self-energies have been presented to describe the pseudogap in cuprates. Here, we offer a derivation of the self-energy in two dimensions due to pair formation and compare it to photoemission data. We then use our results to address several questions of interest, including the existence of magneto-oscillations in the presence of the pseudogap, and the two length scale nature of vortices in underdoped cuprates.

PACS numbers: 74.25.Jb, 74.40.+k, 74.20.Fg

Various models for the self-energy have been presented to describe photoemission spectra for the cuprate pseudogap phase.¹ The basic functional form is

$$\Sigma(k, \omega) = \frac{\Delta^2}{\omega - X_k + i\Gamma_0} \quad (1)$$

where Δ is the energy gap² and Γ_0 the broadening. For the pairing scenario, $X_k = -\epsilon_k$, where ϵ_k is the single particle dispersion. This Ansatz has a long history going back to the original BCS theory,³ where it implicitly describes broadening due to impurities.⁴

Lee, Rice, and Anderson⁵ were able to derive the same functional form for a one-dimensional density wave state, with $X_k = \epsilon_{k+Q}$ where Q is the wavevector of the density wave. In this one dimensional case, long range order is not present ($\Delta^2 \equiv \langle \Delta^2 \rangle$). The result was derived at lowest order restricting to static thermal fluctuations. In this case, Γ_0 is replaced by $\Gamma_2 = v_F/\xi$ where v_F is the Fermi velocity and ξ the correlation length. A similar derivation in two dimensions yields instead⁶

$$-Im\Sigma(k, \omega) = \frac{\Delta^2}{\sqrt{(\omega + \epsilon_k)^2 + \Gamma_2^2}} \quad (2)$$

Eq. 1 was proposed some time ago to describe data in the pseudogap phase of the cuprates.⁷⁻⁹ In Ref. 7, it was motivated by a ‘zero dimensional’ approximation where the fermion dispersion is ignored (i.e., $\epsilon_{k-q} \sim \epsilon_k$) when doing the momentum integration ($\Sigma \sim \int DG$ where D is the boson propagator and G is the fermion Green’s function). In this case, Γ_0 in Eq. 1 reduces to that of time dependent Ginzburg-Landau theory, and should scale approximately as $T - T_c$ (as compared to the $\sqrt{T - T_c}$ behavior of Γ_2 in Eq. 2). This was found to give a good account of the T dependence of the photoemission data above T_c for underdoped cuprates at the antinodal points of the Brillouin zone (where the d -wave energy gap is largest).⁷ It was claimed in this work that this functional form could be motivated in higher dimensions as well, but as we show here, this is dependent on the value of two physical parameters, Δ/T_c and $v_F/\xi_0 T_c$.

Recently, Senthil and Lee¹⁰ proposed a related Ansatz for the zero temperature limit, which was motivated by a desire to address magneto-oscillation data in the

cuprates. Their Ansatz, though, leads to three spectral peaks, as opposed to Eq. 1 that either yields two peaks (gapped case) or one peak (gapless case) depending on the ratio Γ_0/Δ . Their result is similar to a related one derived for a spin density wave by Kampf and Schrieffer.¹¹ We note that both results seem to be at variance with the expectation that the energy gap should be confined to the ordered and ‘renormalized classical’ phases, and therefore should not be present in the zero temperature limit unless ordering is present.¹²

In this Rapid Communication, we provide a derivation of the fermion self-energy due to pairing including both the static thermal fluctuations as in Refs. 5,6 and the dynamical fluctuations as in Ref. 7. Above T_c , we find a result in two dimensions which contains aspects of both Eqs. 1 and 2, with the dynamical broadening (Γ_0) dominating over the thermal broadening (Γ_2) if $v_F/\xi_0\Delta$ is small relative to unity (this ratio is π in BCS theory), where ξ_0 is the bare coherence length. With a reasonable choice of parameters, we find that it quantitatively fits photoemission data for underdoped cuprates. At $T = 0$, we find that for these same parameters, three spectral peaks are indeed present in agreement with the work of Senthil and Lee, though for BCS parameters, only a single peak occurs.

To lowest order, the electron self-energy is obtained by convolving the pair propagator with the hole propagator:

$$\Sigma(k, \omega_n) = -T \sum_m \int \frac{d^d q}{(2\pi)^d} D(q, \Omega_m) G_0(q - k, \Omega_m - \omega_n) \quad (3)$$

where D is the pair propagator and G_0 is the bare Green’s function ($G_0^{-1} = i\omega_n - \epsilon_k$), with the sum over boson Matsubara frequencies. In the BCS approximation, D is $\Delta^2 \delta(q) \delta(\Omega)$, immediately giving rise to Eq. 1 with $\Gamma_0 = 0^+$. In the absence of long range order,

$$D^{-1} = N_0(x + \xi_0^2 q^2 + \alpha|\Omega_m|) \quad (4)$$

with¹³ $x \sim (T - T_c)/T_c$, $\alpha \sim \pi/(8T_c)$ and $\xi_0 \propto v_F/T_c$. N_0 is the density of states per unit cell. For $T > T_c$, the dominant contribution to the Matsubara sum comes from the branch cut of D on the real axis. This leads to

$$(\coth(\Omega/2T) \sim 2T/\Omega)$$

$$\Sigma(k, \omega_n) = \frac{T}{N_0} \int \frac{d^d q / (2\pi)^d}{x + \xi_0^2 q^2} \frac{1}{i\omega_n + i(x + \xi_0^2 q^2)/\alpha + \epsilon_{q-k}} \quad (5)$$

Evaluating (d=2 is assumed from here on), we find

$$\Sigma = \frac{-i\tilde{\Delta}^2}{\sqrt{(\omega + \epsilon_k)^2 + \Gamma_2^2}} \tan^{-1} \frac{\sqrt{(\omega + \epsilon_k)^2 + \Gamma_2^2}}{-i(\omega + \epsilon_k) + \tilde{\Gamma}_0} \quad (6)$$

with $\tilde{\Delta}^2 = \frac{T}{2\pi N_0 \xi_0^2}$, $\Gamma_2 = v_F \sqrt{x}/\xi_0$ and $\tilde{\Gamma}_0 = 2x/\alpha$. Although this formula does a good job of reproducing the filling in of the pseudogap with temperature seen by photoemission, the T dependence of the spectral gap magnitude is not properly reproduced - in particular, the spectral peak position exceeds $\tilde{\Delta}$ in magnitude for a large range of T . This problem can be traced to the definition of $\tilde{\Delta}$ itself. In Ref. 7, this difficulty was avoided in the derivation of Eq. 1 by ignoring the q dependence of the second term in Eq. 5. By making this approximation, this term could be extracted outside the q integral. The q integral then reduces to the definition of the fluctuational gap, $\langle \Delta^2 \rangle$. The issue, though, is that the static terms giving rise to Γ_2 are ignored in this approximation.

These troubles ultimately stem from the fact that Eq. 4 is a low q , low Ω approximation of the true pair propagator. Use of Eq. 4, though, closely matches the exact result if the thermal approximation (\coth replaced by $2T/\Omega$) is used to cut-off the Ω integration, and the q integral is cut-off at $1/\xi_0$.¹⁴ Evaluating Eq. 5 with the cut-off gives

$$\Sigma = -\frac{T}{4\pi N_0 \xi_0^2} \frac{1}{\sqrt{c}} \ln \frac{2\sqrt{c} \sqrt{a + \frac{b}{x+1} + \frac{c}{(x+1)^2}} + \frac{2c}{x+1} + b}{2\sqrt{c} \sqrt{a + \frac{b}{x} + \frac{c}{x^2}} + \frac{2c}{x} + b} \quad (7)$$

where $a = -1/\alpha^2$, $b = -v_F^2/\xi_0^2 + 2i(\omega + \epsilon_k)/\alpha$ and $c = (\omega + \epsilon_k)^2 + xv_F^2/\xi_0^2$. At high frequencies, this reduces to

$$\Sigma_{high} = \frac{T}{4\pi N_0 \xi_0^2 \omega} \ln \frac{x+1}{x} \quad (8)$$

Noting that in this approximation, the fluctuational gap is

$$\langle \Delta^2 \rangle = \frac{T}{4\pi N_0 \xi_0^2} \ln \frac{x+1}{x} \quad (9)$$

we now find the proper high frequency behavior of the self-energy, $\langle \Delta^2 \rangle / \omega$.

Formally, $\langle \Delta^2 \rangle$ has a singular temperature dependence, but for purposes here, we will simply set its value to experiment, noting that photoemission spectra indicate no temperature dependence of Δ at the antinode.⁷ In Fig. 1a, the real and imaginary values of the self-energy from Eq. 7 versus ω are shown for $x = 0.1$, and in Fig. 1b the half width half maximum of the imaginary part is shown versus x . The parameters used were $\Delta/T_c = 4$ and $v_F/\xi_0 T_c = 1$. These values were chosen so as to give

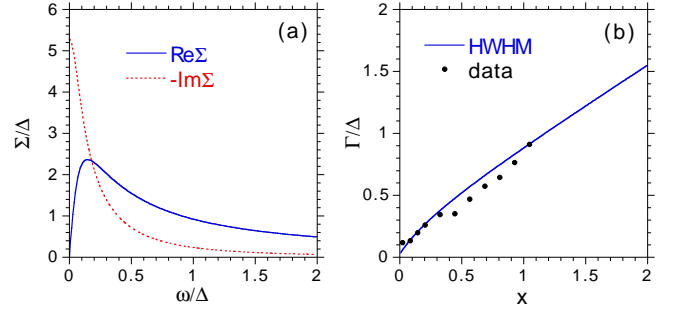


FIG. 1: (Color online) (a) Self-energy from Eq. 7. Parameters are $x \equiv (T - T_c)/T_c = 0.1$, $\Delta/T_c = 4$ and $v_F/\xi_0 T_c = 1$. (b) Half width of $\text{Im}\Sigma$, denoted as Γ , versus x compared to the data of Ref. 7.

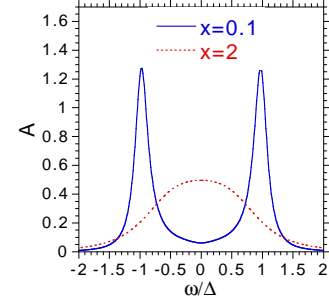


FIG. 2: (Color online) Spectral functions ($\epsilon_k = 0$) using the same parameters as Fig. 1 for $x = 0.1$ and $x = 2$.

a good account of the experimental half width versus x extracted from fitting photoemission data on underdoped cuprates using Eq. 1.⁷ We note that the Δ/T_c ratio of 4 (as compared to the BCS value of 1.76) is a typical value observed in cuprates. The value of $v_F/\xi_0 T_c$ of 1 (as compared to the BCS value of 1.76π) acts to emphasize the dynamic broadening ($\tilde{\Gamma}_0$) over the static broadening (Γ_2). The ratio of these two values is only $1/4$ (compared to the BCS value of π) and will have further consequences as discussed below. As mentioned before, the resulting spectral functions have either two peaks or one peak depending on the magnitude of the half width relative to Δ , with examples shown in Fig. 2. This crossover over from gapped to gapless behavior occurs when the ratio of the half width to Δ is about $\sqrt{2}$, the same as from Eq. 1.

In the zero temperature limit, the imaginary part of the self-energy is given by

$$- \text{Im}\Sigma(k, \omega) = \int \frac{d^d q}{(2\pi)^d} \int \frac{d\Omega}{2\pi} (\text{sgn}(\Omega) - \text{sgn}(\Omega - \omega)) \text{Im}G(\omega - \Omega, k - q) \text{Im}D(\Omega, q) \quad (10)$$

Without cut-offs, this integral is

$$- \text{Im}\Sigma = \frac{1}{4\pi N_0 \xi_0^2} \text{Im} \ln \frac{\frac{\omega + \epsilon_k}{\Gamma_2} - \frac{i\Gamma_2}{\tilde{\Gamma}_0} + \sqrt{1 + \frac{(\omega + \epsilon_k)^2}{\Gamma_2^2}}}{\frac{\epsilon_k}{\Gamma_2} - \frac{i\Gamma_2}{\tilde{\Gamma}_0} + \sqrt{1 + \frac{\epsilon_k^2}{\Gamma_2^2} + \frac{2i\omega}{\tilde{\Gamma}_0}}} \quad (11)$$

where x in Eq. 4 is now a tuning parameter besides temperature - magnetic field, etc., i.e., $(H - H_{c2})/H_{c2}$ - with $x = 0$ corresponding to the quantum critical point where long range order appears.¹⁵ The result is that $-\text{Im}\Sigma$ always grows with frequency, saturating to a constant as $\omega \rightarrow \infty$. The real part of the self-energy can be obtained by numerical Kramers-Kronig,¹⁶ and it is found that the resulting spectral function is gapless. The reason is that formally, the integrals defining $\langle \Delta^2 \rangle$ are divergent, so cut-offs must be invoked, this time not only in momentum, but also in frequency as well. We choose to cut-off the q integral at $1/\xi_0$ and the Ω integral at $1/\alpha$. Reevaluating, we find

$$-\text{Im}\Sigma = \frac{1}{2\pi^2 N_0 \xi_0^2} \text{Im} \int_{q_1}^{q_2} dq_x [c(x+1) \tan^{-1} c(x+1) - c(x) \tan^{-1} c(x)] \quad (12)$$

where $c(y)^{-1} = \sqrt{y + q_x^2 + i\alpha(\omega - v_F q_x/\xi_0)}$, $q_1 = \max(0, (\omega - 1/\alpha)\xi_0/v_F)$ and $q_2 = \min(\omega\xi_0/v_F, 1)$ with q now expressed in units of $1/\xi_0$. Similarly, we find that

$$\langle \Delta^2 \rangle = \frac{1}{8\pi^2 N_0 \xi_0^2 \alpha} [(x+1) \ln \frac{(x+1)^2 + 1}{(x+1)^2} - x \ln \frac{x^2 + 1}{x^2} + 2 \tan^{-1}(x+1) - 2 \tan^{-1}(x)] \quad (13)$$

$\langle \Delta^2 \rangle$ is then used to set the prefactor in Eq. 12. We can now evaluate $-\text{Im}\Sigma$ by doing one numerical integration. We note that in this approximation, $-\text{Im}\Sigma$ vanishes beyond a frequency $\omega_c = 1/\alpha + v_F/\xi_0$ due to the cut-off in Ω . In fact, we note that the various cut-offs define two other frequency scales as well, $\omega_1 = 1/\alpha$ and $\omega_2 = v_F/\xi_0$, with ω_c being their sum. ω_1 is associated with the dynamic part of the pair propagator, and ω_2 with the static part.

In Fig. 3a, we plot the self-energy from Eq. 12, and in Fig. 3b the resulting spectral function, for the same parameters as in Fig. 1a. One clearly see the existence of three spectral peaks. We can contrast this behavior with that in Fig. 4, where we show the same as Fig. 3, but now for BCS parameters. In the latter case, the asymptotics of the self-energy sets in at a frequency beyond Δ , and therefore no spectral gap emerges. Similar results are obtained if one replaces the propagator in Eq. 4 by that in a magnetic field in the lowest Landau level approximation.

Our $T=0$ results can be compared to the recent work of Senthil and Lee,¹⁰ where a separable approximation for the propagator was used. In their work, a propagating form was considered

$$\text{Im}D = \frac{\Delta^2 \pi^2 \xi^{-1}}{(q^2 + \xi^{-2})^{3/2}} (\delta(\Gamma - \Omega) - \delta(\Gamma + \Omega)) \quad (14)$$

The resulting self-energy at $T = 0$ is equivalent to that for electrons coupled to an Einstein mode with frequency Γ .³ That is ($\omega > 0$)

$$-\text{Im}\Sigma = \frac{v_F}{2\xi} \frac{\Delta^2 \Theta(\omega - \Gamma)}{(\omega + \epsilon_k - \Gamma)^2 + v_F^2 \xi^{-2}} \quad (15)$$

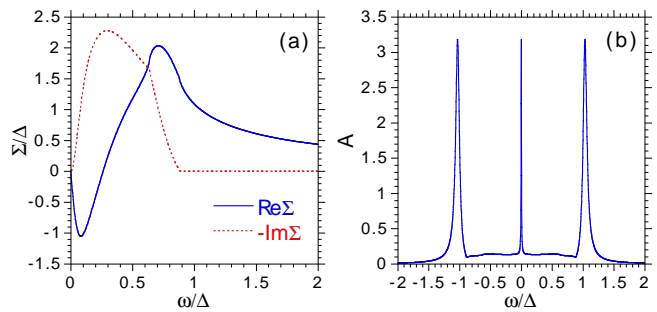


FIG. 3: (Color online) (a) Self-energy from Eq. 12. Parameters are $x = 0.1$, $\Delta/T_c = 4$ and $v_F/\xi_0 T_c = 1$. (b) Spectral function ($\epsilon_k = 0$), where a constant 0.1Δ has been added to $-\text{Im}\Sigma$ so as to resolve the delta functions.

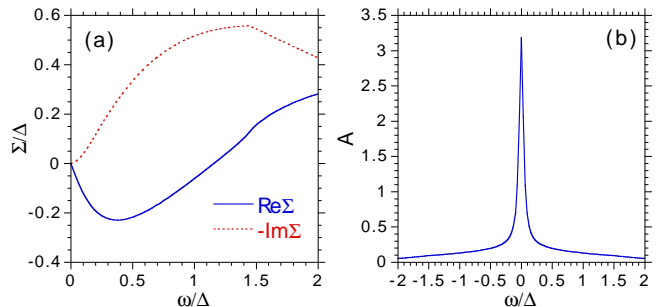


FIG. 4: (Color online) Same as Fig. 3, but for $\Delta/T_c = 1.76$ and $v_F/\xi_0 T_c = 1.76\pi$.

where Θ is the step function. This has a gap between $-\Gamma$ and $+\Gamma$ (with the real part of the self-energy diverging logarithmically at $\pm\Gamma$). As a consequence, the spectral function consists of incoherent peaks at $|\omega| > \Gamma$, and a quasiparticle pole within this gap.

A similar result occurs if one assumes a diffusive behavior which is more appropriate for the disordered phase

$$\text{Im}D = -\frac{2\Delta^2 \pi \xi^{-1}}{(q^2 + \xi^{-2})^{3/2}} \frac{\Omega}{\Gamma^2 + \Omega^2} \quad (16)$$

The resulting self-energy at $T = 0$ is ($\epsilon_k = 0$)

$$-\text{Im}\Sigma = \frac{\Gamma \Delta^2}{\pi(4\Gamma^2 + \omega^2)} \left(\frac{\omega}{\Gamma} \tan^{-1} \left(\frac{\omega}{\Gamma} \right) + \ln \left(1 + \frac{\omega^2}{\Gamma^2} \right) \right) \quad (17)$$

where we have used that $\Gamma = v_F/\xi$. This functional form (Fig. 5a) also leads to a spectral function with three peaks (Fig. 5b).

It is interesting to note that in the Senthil and Lee formalism, the only energy scale is Γ , and therefore a spectral gap occurs as long as the ratio of Γ to Δ is not too large. One reason for the difference from our work is that in their separable approximation, Γ is independent of q , whereas from Eq. 4, one finds that the relaxational rate is strongly q dependent, that is $\Gamma_q = \alpha^{-1}(x + \xi_0^2 q^2)$.¹⁷ We also note that formally, the Ω integral of Eq. 16 is logarithmically divergent when used to define $\langle \Delta^2 \rangle$, but

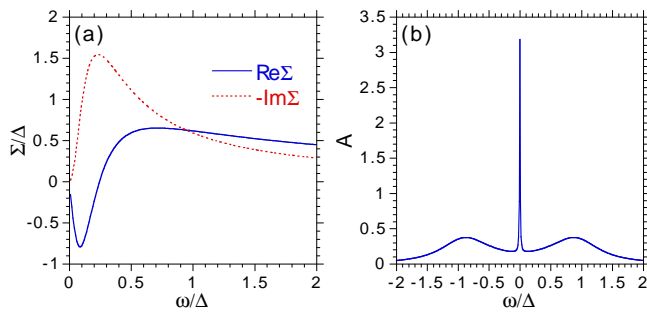


FIG. 5: (Color online) (a) Self-energy from Eq. 17, with $\Gamma = 0.1\Delta$. (b) Spectral function ($\epsilon_k = 0$), where a constant 0.1Δ has been added to $-\text{Im}\Sigma$ so as to resolve the quasiparticle pole.

when calculating the self-energy, this is compensated for by the convergence of the q integral in this separable approximation. That is, Eq. 17 is well behaved without the need to explicitly invoke cut-offs.

We now turn to the question of the electron pockets observed by quantum oscillation experiments.¹⁸ How can such pockets survive in the presence of a large pseudogap, since these electron pockets should originate in the antinodal regions of the zone?¹⁹ As Senthil and Lee point out,¹⁰ as one indeed finds a central peak inside the gap in the low temperature limit, the existence of magneto-oscillations is not a surprise (though in our case, we find a spectral gap only if the asymptotics of the self-energy sets in below Δ). More generally, quantum oscillations are seen in type II superconductors, sometimes for fields much less than H_{c2} . At a semiclassical level, this can be understood since the expectation value of the superconducting order parameter averages to zero over a cyclotron

orbit due to phase winding around the vortices. As a consequence, type II superconductors are gapless at high magnetic fields, with the energy gap causing a broadening of the Landau levels. Quantum mechanical simulations have demonstrated the evolution of the low energy vortex core bound states into Landau levels as the field is increased,²⁰ and similar calculations have been used to address the quantum oscillation data in the cuprates.²¹ Extension of these methodologies to a potential vortex liquid phase above the resistive H_{c2} would be illuminating. We remark that the gapless peak in our work (and Senthil and Lee's) traces out a large Fermi surface, and therefore density wave formation would have to be invoked to explain the small electron pockets that are actually observed.²²

We note that for the parameters in Figs. 1-3, the value of $v_F/\pi\Delta$ is smaller than ξ_0 by a factor of 4π . If we identify the former with the size of the vortex core and assume a typical value of 30 \AA , then the latter is approximately 400 \AA . Such a long length has been identified from terahertz conductivity measurements,²³ and implies a large 'halo' which exists around the vortex cores, leading to the concept of cheap, fast vortices, with the resistive H_{c2} where these halos overlap.^{10,24} Therefore, a large Δ/T_c ratio and a small $v_F/\xi_0\Delta$ ratio are conducive to obtain an extended regime above T_c and H_{c2} where an energy gap exists without long range order, a regime that should be characterized by fluctuating vortices.

Work was supported by the U.S. DOE, Office of Science, under Contract No. DE-AC02-06CH11357. We thank Mohit Randeria, Todadri Senthil and Patrick Lee for discussions.

¹ M. R. Norman, A. Kanigel, M. Randeria, U. Chatterjee and J. C. Campuzano, Phys. Rev. B **76**, 174501 (2007).
² Δ implicitly depends on k , i.e. Δ_k . This is allowed under the assumption that the pair wavefunction factorizes as a product of relative and center of mass degrees of freedom.
³ J. R. Schrieffer, *Theory of Superconductivity* (W. A. Benjamin, New York, 1964).
⁴ A. A. Abrikosov and L. P. Gor'kov, J. Exp. Theor. Phys. **12**, 1243 (1961).
⁵ P. A. Lee, T. M. Rice and P. W. Anderson, Phys. Rev. Lett. **31**, 462 (1973).
⁶ K. Maki, Physica C **282-287**, 1839 (1997).
⁷ M. R. Norman, M. Randeria, H. Ding and J. C. Campuzano, Phys. Rev. B **57**, R11093 (1998).
⁸ M. Franz and A. J. Millis, Phys. Rev. B **58**, 14572 (1998).
⁹ J. Maly, B. Janko and K. Levin, Phys. Rev. B **59**, 1354 (1999).
¹⁰ T. Senthil and P. A. Lee, Phys. Rev. B **79**, 245116 (2009).
¹¹ A. P. Kampf and J. R. Schrieffer, Phys. Rev. B **42**, 7967 (1990).
¹² Y. M. Vilks, Phys. Rev. B **55**, 3870 (1997); Y. M. Vilks and A.-M. S. Tremblay, J. Phys. I France **7**, 1309 (1997).

¹³ M. Tinkham, *Introduction to Superconductivity*, 2nd ed. (McGraw-Hill, 1996).
¹⁴ For similar considerations in the case of magnetism, see G. G. Lonzarich and L. Taillefer, J. Phys. C **18**, 4339 (1985).
¹⁵ We assume that the inclusion of pair breaking (represented by x) leads to a functional form for D equivalent to Eq. 4.
¹⁶ The Kramers-Kronig is performed by linearizing $\text{Im}\Sigma$ over small intervals, each of which is then analytically integrated and summed.
¹⁷ W. J. Skocpol and M. Tinkham, Rep. Prog. Phys. **38**, 1049 (1975).
¹⁸ N. Doiron-Leyraud, C. Proust, D. LeBoeuf, J. Levallois, J.-B. Bonnemaison, R. Liang, D. A. Bonn, W. N. Hardy and L. Taillefer, Nature **447**, 565 (2007).
¹⁹ P. A. Lee, Rep. Prog. Phys. **71**, 012501 (2008).
²⁰ M. R. Norman, A. H. MacDonald and H. Akera, Phys. Rev. B **51**, 5927 (1995).
²¹ K.-T. Chen and P. A. Lee, Phys. Rev. B **79**, 180510(R) (2009).
²² A. J. Millis and M. R. Norman, Phys. Rev. B **76**, 220503(R) (2007).
²³ J. Orenstein, J. Corson, S. Oh and J. Eckstein, Ann. Phys.

15, 596 (2006).

²⁴ P. A. Lee, N. Nagaosa and X.-G. Wen, Rev. Mod. Phys.

78, 17 (2006).